NASA TECHNICAL MEMORANDUM

NASA TM X-52791

NASA TM X-52791

APPLICATION OF HEAT PIPES TO A NUCLEAR AIRCRAFT PROPULSION SYSTEM

by Richard L. Puthoff
Lewis Research Center
Cleveland, Ohio

and

Calvin C. Silverstein
Engineering Consultant
Baltimore, Maryland

TECHNICAL PAPER proposed for presentation at Sixth Propulsion Joint Specialists Conference sponsored by the American Institute of Aeronautics and Astronautics
San Diego, California, June 15-19, 1970

APPLICATION OF HEAT PIPES TO A NUCLEAR AIRCRAFT PROPULSION SYSTEM

by Richard L. Puthoff

Lewis Research Center
Cleveland, Ohio

and

Calvin C. Silverstein

Engineering Consultant
Baltimore, Maryland

TECHNICAL PAPER proposed for presentation at

Sixth Propulsion Joint Specialists Conference
sponsored by the American Institute of Aeronautics and Astronautics
San Diego, California, June 15-19, 1970

NATIONAL AERONAUTICS AND SPACE ADMINISTRATION

APPLICATION OF HEAT PIPES TO A NUCLEAR AIRCRAFT PROPULSION SYSTEM

by Richard L. Puthoff*

Lewis Research Center
National Aeronautics and Space Administration
Cleveland, Ohio

and Calvin C. Silverstein
Engineering Consultant
Baltimore, Maryland

ABSTRACT

A preliminary study was conducted to determine the feasibility of using heat pipes in a nuclear aircraft propulsion system. Heat pipes were the sole transporter of heat. Three sodium coolant heat pipe systems were used. One transferred the heat from the reactor. Another transferred the heat to the air in the jet engine. The third heat pipe transferred the heat from the reactor heat pipe to the jet engine heat pipe. To get promising performance, the technology had to be pushed to the limit.

INTRODUCTION

Many studies have been conducted where heat pipes are applied to nuclear reactor cores or thermionic energy conversion devices. These studies indicate promising advantages in efficiency, design simplification, and weight reduction.

A successful design of a nuclear aircraft propulsion system must meet all specifications of performance and safety at a minimum weight. Heat pipes utilized for removing core heat may reduce system weight by eliminating the need for heavy pumps and high pressure piping. In addition, the system reliability may be improved by the elimination of moving parts and the reduction of system temperature differences about the loop.

This paper presents a preliminary study of heat pipe application for nuclear aircraft propulsion systems[1,2]. The purpose of this study is to show the conceptual design features of a system which uses heat pipes for transferring of reactor core heat to the engine heat exchangers.

In the powerplant design concept used as the basis for this study, a single fast reactor located above the aircraft fuselage powers four jet engines which are mounted below the aircraft wings. The reactor and most of the radiation shield are completely enclosed by a containment vessel. This vessel is capable of absorbing impact forces due to crash landings.

Heat generated in the reactor is transferred to many small diameter heat pipes which penetrate the reactor core. The heat is then transferred from the reactor heat pipes to four large diameter heat pipes, each of which extends between the reactor and one jet engine. At the jet engines, heat is transferred from the large transport heat pipes to compressor discharge air via an array of small-diameter heat pipes similar to those of the reactor. Sodium was used as the fluid for all heat pipes.

Conceptural designs of the reactor, engine, and reactor to engine heat pipes are presented and the amount of U^{235} required for criticality is estimated. The following heat pipe characteristics are defined: wick pore size, wick thickness, heat pipe diameter and length, vapor flow area, axial and radial heat flux; and temperatures of liquid, vapor, and structural materials. The factors that limit the heat pipe performance or dictate the design are identified. Design features that stretch the state-of-the-art are pointed out.

REACTOR TO JET ENGINE HEAT TRANSPORT SYSTEM

The C5-A type aircraft, shown in Fig. 1, was used as a model for estimating elevations and distances between the components of the heat transport system. These components are shown in Fig. 2. They are a nuclear reactor, a reactor heat exchanger, an adiabatic heat transport pipe, and an engine heat exchanger. The reactor, surrounded by a containment vessel, is located on top of the fuselage as shown in Fig. 1.

The nuclear reactor core is cylindrical. It consists of heat pipe fuel elements surrounded by four-inch-thick side and end reflectors (see Fig. 3). The heat pipes consist of a fluid, wick, and tube. The part of the heat pipe within the core is surrounded by an annulus of fuel which in turn is surrounded by cladding. This fueled portion covers about half of the active length of the heat pipe. The heat pipe fuel elements are clustered tightly such that nominally zero spacing occurs between their outer diameters within the active core region. The total heat generation rate is 300 MW.

The heat pipes in the core terminate in the reactor heat exchanger just outside of the end reflector. Two reactor heat exchangers are used, each handling 150 MW. Dual-wicked heat pipes with both external and internal wicks are used as shown in Fig. 4. The external wick extends into the vapor space of the reactor heat exchanger and is connected to the wick which lines the heat exchanger walls. Reactor heat evaporates the sodium liquid in the core. The sodium vapor formed condenses in the zone opposite the external wick. The heat of condensation which is released causes the evaporation of sodium liquid in the external wick.

The sodium vapor formed in each reactor heat exchanger travels down two adiabatic heat transport pipes to the heat exchangers which feed the inboard and outboard engines on one wing. Each pipe is sized to transport a thermal load of 75 MW. The pipe to the outboard engine is 100 ft long and

*Nuclear Engineer.

that to the inboard engine is 65 ft long. There are three right-angle bends in each heat transport pipe. The adiabatic heat transport pipe wall and wick are connected directly to the wall and wick of the engine heat exchangers.

The engine heat exchanger configuration is shown in Fig. 5. Three cylindrical walls divide the exchanger into two flow passages. The inner wall permits passage of the engine shaft and also serves as the inner wall of the compressed air flow passage. The next cylindrical wall separates the compressed air flow passage from that provided for sodium vapor. The outer wall confines the vapor flow, and merges with the adiabatic heat transport pipe. Dual-wicked heat pipes (see Fig. 4) extend radially across the sodium vapor into the compressed air flow passage. Sodium vapor condenses on the outer wick of these heat pipes. The condensate then flows along the heat exchanger to the adiabatic heat transport pipe. Thus, a continuous path is provided for the flow of sodium vapor from the reactor to the jet engines and for the flow of liquid sodium (via the wick flow passage) from the engines to the reactor.

The heat of condensation which is released to the radial heat pipes of the engine heat exchangers vaporizes sodium in the inner pipe wicks of the dual wicked heat pipes. The vapor formed condenses in the section of the heat pipes which lie within the compressed air flow passage. The heat of condensation released at this point is transferred to the compressed air stream which flows over the heat pipes.

The principal design criteria for this study are listed in Table I. Liquid metal property data was obtained from Refs. 3 to 6. The reactor power level is 300 MW. This thermal power is sufficient for powering aircraft with gross weights of 1,000,000 lb.

REACTOR CORE

In designing the reactor core, the size and total number of heat pipes required were calculated first. Then, using the specifications of Table II, the core diameter, fuel element radial temperature gradient, fuel loading, and enrichment were calculated.

Design of Heat Pipes Within the Core

The core heat pipes are closed tubes whose internal surfaces are lined with a porous structure called the capillary wick. The pores of the wick are filled with a liquid, whose vapor occupies the remaining internal volume. The heat generated in the fuel (Fig. 3) is conducted across the heat pipe wall and wick to the liquid-vapor interface, along the tube to a region where heat is being removed from the outer surface of the heat pipe, whereupon the vapor condenses at the liquid-vapor interface. The condensate formed then travels through the wick to the heat addition zone, where it once again evaporates.

All of the heat pipes in the heat pipe heat transport system utilize a two-layer wick, consisting of a liquid flow annulus next to the tube wall and a porous sheet between the liquid flow annulus and the internal vapor space.

The maximum rate at which heat may be transported through a heat pipe is called the heat transport capacity. The heat transport capacity is a function of various relationships. These functional relationships may be described in terms of five heat transport limits; the sonic limit, isothermal limit, entrainment limit, boiling limit and capillary pumping limit. The heat transport capacity of a given heat pipe under given operating conditions will be equal to the lowest heat transport limit corresponding to these conditions. For the core heat pipes, the entrainment limit was the prime limiting design consideration. Entrainment limit is reached when the high velocity vapor flowing over the liquid disrupts the liquid-vapor interface and entrains liquid in the vapor.

The total heat pipe cross-sectional area should be as small as possible to minimize the volume of void and nonfissile material in the reactor core. The heat pipe fluid selected, therefore, must be the highest heat transport capacity per unit cross-sectional area of fluid and vapor. Since the vapor space occupies most of the cross-sectional area in a two layer wick heat pipe, the axial heat flux based on vapor space area is used for the evaluation of heat pipe fluids.

The heat transport capacity, based on the entrainment limit, is given by the following equation

$$\xi_a = \left(\frac{\sigma \rho_v K^2}{C_d D_p} \right)^{1/2} \qquad (1)$$

where ξ_a is the axial heat flux for no entrainment based on the vapor space cross-sectional area, σ is the liquid surface tension, ρ_v is the vapor density, K is the heat of vaporization, D_p is the wick pore diameter, and C_d is an experimentally-determined drag coefficient.

The entrainment axial heat flux can be calculated from Eq. (1) if the drag coefficient C_d is known. Kemme[7] has reported entrainment limit data for a 10 micron diameter wick in a sodium heat pipe, from which C_d can be estimated. Kemme suggested that $C_d D_p = 5 D_p$, from which $C_d = 5$. However, a better fit to his data is obtained if $C_d = 3.33$ in Eq. (1), then

$$\xi_a = (0.447 \text{ to } 0.548) \left(\frac{\sigma \rho_v K^2}{D_p} \right)^{1/2} \qquad (2)$$

In Fig. 6, limiting axial heat fluxes for no entrainment and an evaporator temperature drop not in excess of 20° F are plotted as a function of heat pipe temperature for sodium, potassium, cesium and lithium liquid metals. The limiting axial heat flux based on entrainment is about 50% of the axial heat flux at the sonic limit.

The entrainment limits of Fig. 6 are based upon the lower value of Eq. (2) and have been determined for wick pore diameters of 2 microns and 20 microns. Since preliminary calculations indicated that axial heat fluxes well in excess of 100 kW/in.^{2} would be required, only sodium and potassium are considered and wick pore diameters smaller than 20 microns are required. Since the axial heat flux limit for sodium is higher than for potassium for both the 2-micron and 20-micron pore diameters over the temperature range 1630°-2100° F, sodium was selected as the preferred heat pipe

fluid. (The final operating temperature was 1900° F resulting in an axial heat flux limit of 220 kW/in.^{2}.)

Heat pipe parameters of interest include the vapor space diameter D_v, the temperature drop across the sodium annulus per unit of thickness $\Delta T/ta$, the heat transport rate per heat pipe Q, and the number of heat pipes needed for removal of reactor-generated heat N. In Fig. 7 D_v, $\Delta T/t_a$, Q, and N/2 are plotted as a function of the surface heat flux q_s for a reactor thermal power of 300 MW, sodium heat pipes at 1900° F, and evaporator (in-core) length of 15 in., and a wick pore diameter of 2 microns. The reactor power distribution was assumed to be flat.

Figure 7 indicates that operation at a surface heat flux of about 4 kW/in.^{2} would require 800 heat pipes with a vapor space diameter of 1.1 in. for each half of the reactor core. The thermal power rating per heat pipe would be 205 kW (assuming an axial heat flux limit of 220 kW/in.^{2}), and the temperature drop across the annulus would be 5.5°F/mil. This temperature drop, however, was considered to be excessive. The annular gap thickness was expected to be on the order of 10 mils and the temperature drop across the annulus would be encountered at both the heat input and output regions of the heat pipes.

Therefore, the decision was made to use smaller diameter heat pipes at the expense of a larger number. A vapor space diameter of 0.5 in. was selected, for which the surface heat flux is 1.85 kW/in.^{2}. A total of 3700 of these heat pipes are required for each half of the reactor core, each heat pipe being rated at 45 kW. The total vapor space cross-sectional area of the heat pipes in each half of the core is then 4.8 ft^2, and the temperature drop across the sodium annulus is 2.5° F/mil.

A preliminary estimate of the core diameter indicated that 3700 tubes would result in a core diameter in excess of 45 in. Therefore, a significant increase in the axial heat flux was necessary. The increase was accomplished by (1) increasing the heat pipe temperature to 2000° F, and (2) using the higher of the two values for the entrainment limit (Eq. (2)). The result was a maximum allowable axial heat flux of 307 kW/in.^{2} at a 0.5 in. diameter vapor space and an in-core length of 20 in. The total number of heat pipes using an average power level of 279 kW/in.^{2} was then 2740 for one-half of the core or 5480 for the entire core.

The thickness of the liquid annulus in the reactor heat pipes was established from both boiling limit and capillary pumping limit considerations. The minimum diameter of curvature D_c of the liquid-vapor interface in the wick pores for which boiling will not occur was determined from the following equation:

$$\frac{4\sigma(T_v)}{D_c} \leq \frac{4\sigma(T_w)}{D_n} - \left[P_v(T_w) - P_v(T_v)\right] \qquad (3)$$

where D_c is the diameter of curvature of the liquid-vapor interface, D_n is the diameter of nucleation sites at which vapor bubbles can form, σ is the liquid surface tension, P_v is the vapor pressure, T_v is the vapor temperature in the vapor space, and T_w is the temperature at the inner surface of the heat pipe wall. D_c was taken to be equal to the wick pore diameter of 2 microns. A value of 40° F was assumed for $T_w - T_v$.

The calculated value of D_c was then used with the appropriate capillary pumping limit equation from Ref. 1 to establish a liquid sodium annulus thickness of about 10 mils. In calculating the annular thickness a total heat pipe length of 48 in. was used, consisting of a 20 in. evaporator section, a 7 in. adiabatic section, and a 21 in. condenser section.

The final step for sizing the heat pipes was the determination of the overall heat pipe diameter. This diameter is comprised of the vapor space diameter, wick thickness, the liquid annular thickness, and the heat pipe wall thickness. As indicated above, a vapor space diameter of 0.5 in. was specified. A thickness of 5 mils was arbitrarily selected for the porous wick adjacent to the vapor space. The annular liquid thickness was calculated to be approximately 10 mils. The heat pipe wall was sized at 33 mils. Then the outer diameter of the heat pipe is equal to 0.596 in.

TZM molybdenum was selected as the wall and wick material. Its strength for 0.5% creep in 10,000 hr is 22,000 psi when operating at 2000° F. The material is also compatible with sodium at this temperature. A summary of the final reactor heat pipe design is as follows:

Heat pipe fluid	Sodium
Maximum vapor temperature, °F	2000
Maximum axial heat flux, kW/in.^{2}	307
Average axial heat flux, kW/in.^{2}	279
Vapor space diameter, in.	0.5
Wick pore diameter, microns	2
Wick pore thickness, mils	5
Liquid annulus thickness, mils	10
Heat pipe wall thickness, mils	33
Heat pipe diameter, in.	0.596
Evaporator length, in.	20
Number of heat pipes/half core	2740
Wick and wall material	TZM

Core Diameter

The active core diameter is dependent upon the number of heat pipes, fuel thickness, and cladding thickness. Since the fuel and cladding thickness have been assumed (Table II) the core diameter has in effect been dictated by the 2740 required tubes/half core.

Figure 8 presents the proposed design of the heat pipe fuel element. The area of this hexagonal cell may be calculated as follows:

$$A_{cell} = \frac{\sqrt{3}}{2}(2r_6 + S_r)^2 \qquad (4)$$

where S_r is the radial spacing between heat pipes and r_6 is the radius as shown in Fig. 8. Multiplying Eq. (4) by the number of heat pipes N gives the active core area if the scallops of the outer perimeter are neglected.

$$A_{core} \approx \frac{N\sqrt{3}}{2}(2r_6 + S_r)^2 \qquad (5)$$

From Eq. (5) the diameter of the core is

$$D_{core} = \sqrt{\frac{4}{\pi} A_{core}} = \sqrt{\frac{4}{\pi}\frac{\sqrt{3}}{2} N(2r_6 + S_r)^2} \qquad (6)$$

In terms of fuel thickness t_f and cladding thickness t_{cl}, Eq. (6) becomes

$$D_{core} = \sqrt{\frac{2\sqrt{3}}{\pi} N(2r_4 + 2t_f + 2t_{cl} + S_r)^2} \quad (7)$$

Finally, for an assumed t_{cl} of 0.035 in., an assumed t_f of 0.075 in., a S_r of 0, and 2740 tubes, the core diameter is 45 in. This value meets the maximum core diameter design specification. A smaller core diameter could be obtained by reducing the clad and/or fuel thickness or by making the fuel cross sectional geometry hexagonal instead of circular.

Heat Pipe Fuel Element Radial Temperature Gradient

The heat removed by the heat pipes is generated in the UN fuel surrounding the heat pipe. This internal heat generation and resultant radial flux results in a radial temperature gradient through the heat pipe wall and fuel. No temperature gradient exists in the cladding since no heat is transferred.

The total temperature gradient from the fuel outer wall to the heat pipe inner wall is

$$\Delta t = t_5 - t_3 = \frac{A_o}{4}\left\{\left[\frac{(r_4^2 - r_5^2)}{K_f}\right] + \frac{2r_5^2 \ln(r_5/r_4)}{K_f} + \frac{2 \ln(r_4/r_3)(r_5^2 - r_4^2)}{K_{cl}}\right\} \quad (8)$$

where r_3, r_4, and r_5 are the radii as shown in Fig. 8, A_o is the internal heat generation rate, K_f is the thermal conductivity of the fuel and K_{cl} is the thermal conductivity of the clad.

A radial heat flux of 0.88×10^6 Btu/hr-ft^2 results in a ΔT of 200° F. For a maximum heat pipe vapor temperature of 2000° F the resultant clad temperature is 2200° F.

For TZM at 2200° F the 10,000 hr creep-rupture stress is about 10,000 psi. Since, the clad has no thermal gradients (no heat is lost radially outward) its stresses would be limited to that of fuel swelling, fuel growth, etc. The operating temperature and allowable stresses, therefore, were considered as acceptable.

Fuel Loading

The 0.075 in. thick fuel surrounding each heat pipe also sets the total fuel loading of the core. With the reactor core required to operate for 10,000 hr at 300 MW, the amount of fuel that will be used can be calculated as follows:

300×10^6 Watts × 10,000 hr × 3600 sec/hr

10.8×10^{15} Watt-sec

For U^{235} fuel the burnup rate is 1.452×10^{-11} g U^{235}/watt-sec of operation. The total amount of fuel used is

10.8×10^{15} Watt-sec × 1.452×10^{-11} g U^{235}/Watt-sec

= 157 kg

A fuel thickness of 0.075 in. for the 5480 fuel elements in the core results in a core loading of 3770 kg. The burnup is then (157/3770) × 100 = 4.2%, which is less than the maximum allowable burnup of 5%.

Core Criticality Calculations

The code used in the neutronic analysis was a two-dimensional discrete angular segmentation transport program referred to as TDSN[8]. It is a numerical iterative finite difference method in which the continuous angular distribution of neutron velocities is represented by considering discrete angular directions. The output of the transport program includes the core multiplication factor and the integrated power ratio and flux shapes for each energy group.

A required input to the TDSN transport program are the core cross sections. Multigroup cross sections used in this analysis were obtained from GAM II and GATHER II programs[9,10]. These are then converted to macroscopic cross sections by a Lewis Research Center written code entitled MACROS.

For the calculations the core was divided into one radial zone and one axial zone. Seven group microscopic cross sections were obtained from the GAM II and GATHER II programs over the energy ranges presented in Table III. The macroscopic cross sections calculated by MACROS used the atom densities listed in Fig. 8. A P_0 approximation for neutron scattering and a S_2 discrete angle approximation were used in the neutronic calculations. The core K_{EFF} was calculated over a large range of enrichments. For each fuel enrichment the core atom densities were readjusted. The results of these calculations are presented in Fig. 9, core K_{EFF} as a function of Percent Fuel Enrichment. The required core K_{EFF} was achieved at a 37.5% fuel enrichment.

The normalized power distribution is plotted in Fig. 10. The plot shows that the radial peak to average power ratio is about 1.5 compared to a desired 1.1. Since the fuel enrichment is low, however, fuel zoning could be accomplished to better meet this requirement. The low flux at the boundary also results in a low radial neutron leakage of 10%. This would not permit the use of a reflector control system such as reflector control drums. However, if the radial power distribution were flattened to nearer the 1.1 ratio the radial leakage would increase and reflector control may then be feasible.

A summary of the core calculations is as follows:

Core diameter (0.075 in fuel, 0.035 in clad), in.	45
Fuel enrichment, percent	37.5
Fuel loading, kg	3770
Clad temperature, °F	2200
Maximum allowable clad stress, psi	10,000
Core K_{EFF}	1.1

In Table IV the diameter of the heat pipe cooled fast core is compared with the diameters of a liquid sodium cooled fast core and a helium cooled thermal core. The cores were all designed for the same power level and operating lifetime. The fuel burnups are also indicated in Table IV. The heat pipe cooled core is seen to be intermediate in size between the others, although absolute comparisons are not possible because the fuel burnup is different in each core. If the fuel loading of the heat pipe cooled core were reduced suffi-

ciently to raise the burnup to 10%, the core diameter could be reduced to 39 in. The core K_{EFF} of 1.1 would then be maintained by an increase in the fuel enrichment to offset the reduction in the total fuel loading.

The scope of this study did not include the design of control rods or drums. The calculated boundary neutron flux and radial leakage however, indicate that control drums would be difficult to apply. Therefore, a more optimized design should endeavor to flatten the radial power distribution, reduce the core diameter, or incorporate poison heat pipe tubes within the core.

REACTOR HEAT EXCHANGERS

A reactor heat exchanger enclosure is shown in Fig. 11. The condensing, dual-wicked sections of the reactor heat pipes extend from the reactor face into the cylindrical section. The interior walls are lined with a two-layer wick consisting of a 0.300 in. thick liquid sodium flow channel and a 30 mil thick TZM wick of 30% porosity. The enclosure wick is connected with the external wicks of the heat pipes, so that liquid sodium can flow freely into the external wicks of the reactor heat pipes (see Fig. 12).

The reactor heat exchanger has two exit flow passages, each of which connects to an adiabatic heat transport pipe. The cross-sectional area of the vapor space in each rectangular exit section is the same as that of the adiabatic heat transport pipe to which it connects. The exit flow passages add 7.80 in. to the heat exchanger length. The total distance from the center plane of the reactor core to the end of one reactor heat exchanger is 47.2 in.

The enclosure walls are fabricated from TZM. (Tantalum alloys may be preferable.) The outer surface is clad with an oxidation-resistant alloy such as Udimet 500. The wall thickness of 0.238 in. was established from buckling rather than stress considerations. This thickness is required to prevent crushing of the enclosure walls by atmospheric pressure when the system is cold and the internal pressure of the sodium vapor is negligible.

As Fig. 12 shows, the outer wick of the heat pipes consists of a 12 mil thick liquid sodium annulus which is surrounded by a 5 mil thick sheet of TZM with 30% porosity. Since the section of heat pipe wall within the heat exchanger enclosure does not have to support any load of significance (the internal and external pressures are almost the same), the thickness of the externally wicked wall was reduced to 16 mils. The overall diameter is then 0.596 in. over the entire heat pipe length.

The design of the internal heat pipe wick was based on a total heat pipe length of 48 in., which included a 7 in. adiabatic section and a 21 in. condensing length. Space limitations within the reactor containment vessel resulted in specification of a total heat pipe length of 39 in., including a 4 in. adiabatic section and a 15 in. condensing section. While the shorter heat pipe length would permit the use of a thinner internal liquid sodium flow passage, the originally calculated thickness of 10 mils was retained.

The surface heat flux in the condensing section of the heat pipes (which lie within the reactor heat exchangers) is 33% greater than that in the evaporator section which lies within the reactor core. The temperature drop between the internal heat pipe vapor in the condensing section and the reactor heat exchanger vapor outside the external heat pipe wicks is 110° F for the highest power heat pipe. For the average heat pipe, the temperature drop is 100° F. The estimated temperature drop in the internal vapor along the heat pipe length is 10° F.

ADIABATIC HEAT TRANSPORT PIPES

The adiabatic heat transport pipes leading to the outboard engines were designed first. The same design was then used for the inboard pipes, from Fig. 13 the outboard adiabatic heat transport pipe is about 100 ft long, and includes three right-angle bends. If it is assumed that the pipe is 20 in. in diameter and a bend radius equal to twice its diameter, then the equivalent length of each bend is 6.9 ft. The total effective pipe length is about 120 ft.

A cross section of the adiabatic heat transport pipe is shown in Fig. 14. The overall diameter is about 21.5 in. The wall and wick are fabricated from TZM molybdenum. The wall is clad externally with an oxidation-resistant superalloy such as Udimet 500. The wick is 30 mils thick, and has a porosity of 30% and a pore diameter of 1.5 microns. The wall thickness of 0.111 in. is a result of the requirement that the wall withstand buckling from the external atmosphere when the pipe is cold and the internal sodium vapor pressure is negligible.

The liquid and vapor pressure distribution in the adiabatic heat transport pipe are shown in Fig. 15. Most of the indicated liquid pressure drop results from the difference in elevation between the reactor heat exchanger and the engine heat exchanger. The static liquid sodium pressure drop of 27.3 psi was calculated for a 30 degree bank and 1.5 g's of vertical acceleration. (The horizontal component of acceleration which acts during a coordinated turn was conservatively neglected. This in effect assumes the airplane is banked while not turning.) The pressure drop calculations were carried out for a thermal load of 67,500 kW, a vapor space diameter of 20 in., and a liquid sodium annulus thickness of 0.752 in. The vapor temperature was 1880° F.

The vapor and liquid in the adiabatic heat transport pipe are contiguous with the vapor and the liquid in the reactor heat exchanger and the vapor annulus of the engine heat exchanger. The axial heat flux (based on vapor space cross-sectional area) is 239 kW/in.^{2} in the adiabatic heat transport pipe and the reactor heat exchanger, and 180 kW/in.^{2} in the vapor annulus of the engine heat exchanger. These fluxes are below the axial flux limits of 261 kW/in.^{2} for a wick pore diameter of 2 microns, and using the upper value of the constant in Eq. (2).

The net pressure drop in the adiabatic heat transport pipe vapor as it travels from the reactor heat exchanger to the engine heat exchanger is

6.7 psi. The associated temperature drop is about 30° F. Therefore, the minimum vapor temperature is 1850° F. The vapor temperature at the entrance to the engine heat exchanger is about 1860° F. Thus, the mean vapor temperature is 1855° F. (The design of the engine heat exchanger was carried out for a mean vapor temperature of 1860° F.)

From Fig. 15, the maximum difference between vapor and liquid pressures is 36.4 psi. A wick pore diameter of 1.58 microns is needed if surface tension is to withstand this pressure difference. This is larger than the wick pore diameter of 1.5 microns which was specified for design purposes.

In the reactor heat pipe of average thermal load, the temperature drop through the external wick is 44° F. The temperature at the wall is then 1890 + 44 = 1934° F. The sodium vapor pressure at this temperature is 54 psi, and the difference between the vapor and liquid pressures is 54 - 8.6 = 45.4 psi. It can be shown that boiling at the external surface (outer surface of the outer wick) will be suppressed only if the nucleation site diameter does not exceed 1.27 microns. Data and equations developed by Chen[11] indicate that the absence of nucleation sites with diameters larger than 1.27 microns can be insured. It is accomplished by pressurizing the adiabatic heat transport pipe to 50 psi or more with subcooled liquid sodium prior to operation.

The above discussion indicates that an adiabatic heat transport pipe with a vapor space diameter of 20 in. and a liquid sodium annulus thickness of 0.752 in. represents a viable design, if the pore diameter of the porous sheet which lines the interior is 1.5 microns.

ENGINE HEAT EXCHANGERS

The principal heat exchanger design factors which were determined include: exchanger dimensions, heat pipe temperatures, and the heat transport capability of the radial heat pipes.

Exchanger Dimensions

The heat exchanger geometric parameters are shown in Fig. 16. The engine shaft passes through the inner cylinder of radius r. Compressor discharge air flows through the inner annulus of width l_a (the heat pipe condensing length). Sodium vapor from the adiabatic heat transport pipe flows circumferentially through the outer annulus of width l_v (the heat pipe evaporating length). The radial heat pipes of diameter d are arranged in n rows, one diameter apart, along the heat exchanger length L. There are n heat pipes per row. The heat pipes in adjacent rows are staggered. The mean spacing between the radial heat pipes in a given row is $\overline{X}_{ta}d$ in the air annulus and $\overline{X}_{tv}d$ in the vapor flow annulus.

The radius r was determined to be 7.0 in. upon application of the design criterion that the cross-sectional area of the engine shaft should not exceed 1/16 the cross-sectional area of the compressor (which had a specified diameter of 4.74 ft).

Dimensions of the air flow passage were determined from parametric studies of the heat transfer rate between the surface of constant temperature heat pipes and the compressor discharge air. Actually, the temperature of the heat pipes varies from row-to-row along the heat exchanger length. The constant temperature used in the analysis therefore represents a mean of the heat pipe surface temperature variation along the heat exchanger length. The analysis was carried out in accordance with the methods of Ref. 12.

The vapor flow annulus was sized on the basis of the frictional pressure drop in the sodium vapor. This must be kept within reasonable bounds in order not to exceed the capillary pumping capability of the adiabatic heat transport pipe. The pressure drop analysis is similar to that for the compressed air, but taking into account the fact that the flowing fluid is a condensing vapor instead of a gas, which splits in half upon entering the heat exchanger, with each half traveling a distance equal to one-half the exchanger circumference before being completely condensed. Calculations were carried out for an assumed heat pipe surface temperature of 1820° F in the air annulus. The temperature of sodium vapor entering the vapor annulus of the heat exchanger was taken to be 1860° F.

The results of the calculations are presented in Fig. 17, where the heat exchanger length L, diameter D, and the total number of heat pipes N are shown as a function of heat pipe diameter. It was decided to limit vapor friction pressure drop to 2.5 psi at a heat pipe diameter D of 0.5 in. The heat pipe diameter in the vapor annulus was assumed to be 30 mils larger than D. Then, from Fig. 17,

Exchanger diameter D = 7.2 ft

Exchanger length L = 4.0 ft

Number of heat pipes N = 8300

For these conditions, the following additional data apply:

Air annulus width l_a = 23.4 in.

Vapor annulus width l_v = 12.8 in.

Total heat pipe length L_p = 36.2 in.

Heat pipe diameter D in vapor annulus = 0.530 in.

Effective axial heat flux in vapor annulus = 110 kW/in.^{2}

Average heat load per heat pipe = 8.13 kW

The outer shell of the vapor annulus is fabricated from TZM, and is externally clad with an oxidation-resistant coating. It is subjected to internal pressure during normal operation (i.e., the sodium vapor pressure) and to external pressure from the atmosphere when the nuclear propulsion system is not operative and is relatively cool. (The sodium vapor pressure, and hence the internal pressure, is then negligible.) The latter condition results in the most severe design condition, and requires a shell thickness of 0.456 in. to prevent buckling of the outer shell by external atmospheric pressure.

The inner shell of the vapor annulus is also fabricated from TZM, and is clad with a few mils of an oxidation-resistant alloy on the inner, air ex-

posed surface. The inner shell is not subjected to external buckling pressures when cold, and hence was designed on the basis of tensile stress arising from internal pressure. In current design concepts, the jet engines are powered by chemical combustors during takeoff and landing. When the engines are operating on chemical fuel, compressor discharge air flows through the inactive engine heat exchangers prior to entering the combustors. At sea level, the compressor discharge pressure is about 350 psi and the temperature is about 750° F. A thicker inner shell is required for this condition than for nominal design conditions at the cruising altitude of 36,000 ft. The required shell thickness, using an allowable stress of 80,000 psi for TZM, is then 0.133 in.

Engine Exchanger Heat Pipes

The dimensions of the engine exchanger heat pipes are shown in Fig. 18. The internal and external wicks are filled with liquid sodium. The external wick is fabricated from TZM with 30% porosity. The heat pipe wall and the internal wick with 30% porosity are fabricated from Udimet 500, a fabricable alloy with good oxidation resistance at contemplated operating temperatures.

The most severe design condition again occurs when the engines are operating on chemical fuel at sea level, when the compressed air is at 350 psi and 750° F. The 12 mil thick wall is then stressed to 7250 psi, which is well below the yield stress of 110,000 psi for Udimet 500. The external pressure of 350 psi is also well below the external pressure of 950 psi which is required for buckling.

The average surface heat flux based on the mean thickness of the heat pipe wall is 0.413 $kW/in.^2$ in the vapor annulus and 0.226 $kW/in.^2$ in the air annulus. The temperature drop through the heat pipe wall and wick is then calculated to be 35° F in the vapor annulus and 14° F in the air annulus. Since the sodium vapor temperature in the vapor annulus is 1860° F, the vapor temperature inside the heat pipes is 1825° F. Neglecting the relatively small vapor temperature drop along the heat pipe length, the heat pipe surface temperature in the air annulus is then 1811° F. A mean surface temperature of 1820° F had been assumed in the calculations for determining the engine heat exchanger dimensions.

The capability of the engine exchanger heat pipe to handle the required heat loads will now be examined. The coldest heat pipes are located at the air inlet of the engine heat exchanger. Since the difference between the surface and air temperatures is a maximum at the air inlet, as indicated qualitatively in Fig. 19, the coldest heat pipes also carry the largest heat load. Since the heat transport capacity of a heat pipe generally decreases with a decrease in temperature, the capability of the coldest heat pipe to carry the imposed heat loads must be established.

An approximate, iterative calculation indicated that the heat load on the coldest heat pipes is about 25.4 kW (compared to the mean heat load of 8.13 kW). The vapor temperature inside the heat pipes is then about 1750° F. The axial flux of 165 $kW/in.^2$ is less than the maximum of 212 $kW/in.^2$ for no entrainment and an evaporator momentum temperature drop of less than 20° F when the wick pore diameter is 2 microns.

The maximum pressure differential across the liquid-vapor interface, including the maximum liquid gravity head of 1.42 psi, was calculated to be 4.80 psi. This is well below the maximum pressure differential of 31.2 psi which can be sustained by the surface tension of sodium in wick pores with a diameter of 2 microns. From Eq. (3) it can be established that boiling will not occur unless nucleation site radii are equal to or greater than 8 microns.

The above data indicate that the design of the engine heat exchangers heat pipes is adequate to handle the imposed heat loads if the wick pore diameter is 2 microns.

CONCLUSIONS

The following conclusions are made based upon the preliminary analysis conducted in this paper.

1. The concept of utilizing heat pipes for the removal of core heat in a 300 MW nuclear aircraft reactor appears promising. However, the required level of heat pipe performance is pushed to the limit of present heat pipe technology. In particular, wick pore diameters of 1.5 to 2 microns are required to achieve the axial heat fluxes which are needed for sufficient compactness of system components.

2. The active core diameter of 45 in. (4.2% burnup) compares with 30 in. for a liquid metal fast reactor (12% burnup) and 62 in. for a water moderated thermal reactor (20% burnup). A smaller core diameter of 39 in. is possible for the heat pipe core if a 10% burnup were assumed.

3. The use of reflector control drums for control of the current design will be difficult due to the reduced neutron flux at the core boundary.

4. The structural material temperatures of 1750° to 2100° F mean that refractory metals will probably be required with attendant difficult problems. All the refractory metals require protection from oxidation. Some are brittle at low temperatures and difficult to fabricate.

REFERENCES

1. Silverstein, C. C., "A Study of Heat Pipe Applications in Nuclear Aircraft Propulsion Systems," SIL-104, NASA CR-72610, Dec. 1969, Silverstein Consultant Engineer, Baltimore, Md.

2. Puthoff, R. L., "Neutronic Design of a Reactor Core Containing Heat Pipes for Application to a Nuclear Airplane," TM X-52765, 1970, NASA, Cleveland, Ohio.

3. Weatherford, W. D., Jr., Tyler, J. C., and Ku, P. M., "Properties of Inorganic Energy-Conversion and Heat-Transfer Fluids for Space Applications," WADD-TR-61-96, Nov. 1961, Southwest Research Institute, San Antonio, Texas.

4. Hoffman, H. W. and Robin, T. T., Jr., "Preliminary Collation of the Thermodynamic and Transport Properties of Cesium," ORNL-TM-1755, NASA CR-88967, June 1967, Oak Ridge National Lab., Oak Ridge, Tenn.

5. Hoffman, H. W. and Cox, B., "A Preliminary Collation of the Thermodynamic and Transport Properties of Potassium," ORNL-TM-2126, NASA CR-96741, July 1968, Oak Ridge National Lab., Oak Ridge, Tenn.

6. Burdi, G. F., "Snap Technology Handbook. Vol. I: Liquid Metals," NAA-SR-8617, May 1964, Atomics International, Canoga Park, Calif.

7. Kemme, J. E., "High Performance Heat Pipes," presented at the IEEE Thermionic Conversion Specialist Conference, Palo Alto, Calif., Oct. 30, 1967.

8. Barber, C. E., "A FORTRAN IV Two-Dimensional Discrete Angular Segmentation Transport Program," TN D-3573, 1966, NASA, Cleveland, Ohio.

9. Jeanou, G. D. and Dudek, J. S., "GAM-II. A B_3 Code for the Calculation of Fast-Neutron Spectra and Associated Multigroup Constants," GA-4265, Sept. 1963, General Dynamics Corp., San Diego, Calif.

10. Jeanou, G. D., Smith, C. V., and Vieweg, H. A., "GATHER-II. An IBM-7090 FORTRAN-II Program for the Computation of Thermal-Neutron Spectra and Associated Multigroup Cross Sections," GA-4132, July 1963, General Dynamics Corp., San Diego, Calif.

11. Chen, J. C., "Incipient Boiling Superheats in Liquid Metals," Journal of Heat Transfer, Vol. 90, No. 3, Aug. 1968, pp. 303-312.

12. Kays, W. M. and London, A. L., Compact Heat Exchangers, 2nd ed., McGraw-Hill, New York, 1964.

Reactor-to-Jet Engine Heat Transport System	
Reactor Thermal Power	300 Mw
Thermal Power Available to Jet Engines	270 Mw
Maximum Temperature of Heat Pipes in Reactor	2100°F
Maximum Reactor Outside Diameter	68 in.
Reactor and Jet Engine Locations	See Figure 1
Maximum Surface Heat Flux of Heat Pipes in Reactor	2×10^6 Btu/ft^2-hr
In-flight Acceleration and Banking Angle	1.5 g's, 30°
Reactor Radial and Axial Peak-to-Average Power Distribution	1.1
Engine Heat Exchanger Inlet Air Temperature and Pressure	540°F, 70 psia
Engine Heat Exchanger Air Outlet Temperature	1450°F
Air Pressure Drop Through Engine Heat Exchanger	10%
Total Air Flow Rate Through Each Engine Heat Exchanger	≈ 275 lb/sec
Length of Engine Heat Exchanger	≤ Compressor Diameter
Maximum Diameter of Engine Heat Exchanger	7 ft
Compressor Diameter	4.74 ft
Cross-Sectional Area of Engine Shaft	≤ 1/16 Cross Sectional Area of Compressor
Cruise Altitude	36,000 ft

TABLE I. - PRINCIPAL DESIGN CRITERIA FOR HEAT PIPE APPLICATIONS STUDY

Core fuel	UN
Clad	TZM Moly
Core K_{EFF}	1.1
Core lifetime, hr	10,000
Peak fuel burnup, %	5
Fuel thickness, in.	0.075
Clad thickness, in.	0.035
Active core diameter, in.	45
Side and end reflector	4 in - Moly
Radial peak to average power ratio	1.1
Axial peak to average power ratio	1.0

TABLE II. - REACTOR CORE DESIGN SPECIFICATIONS

Group	Neutron energy range	
	eV	u
1	1.49×10^{7} to 2.23×10^{6}	-4.00×10^{-1} to 1.5
2	2.23×10^{6} to 8.2×10^{5}	1.5 to 2.5
3	8.21×10^{5} to 7.10×10^{3}	2.5 to 7.25
4	7.10×10^{5} to 7.49×10^{2}	7.25 to 9.50
5	7.49×10^{2} to 29.0	9.50 to 12.80
6	29.0 to 0.414	12.80 to 17.0
7	0.414 to 0	17.0 to ---

TABLE III. - NEUTRON ENERGY GROUPS

Core type	Diameter, in.	Fuel burnup, %
Heat pipe-cooled fast	45	4.2
Liquid sodium-cooled fast	30	12
Helium-cooled thermal (water moderated)	62	20

TABLE IV. - COMPARISON OF CORE TYPES

E-5650

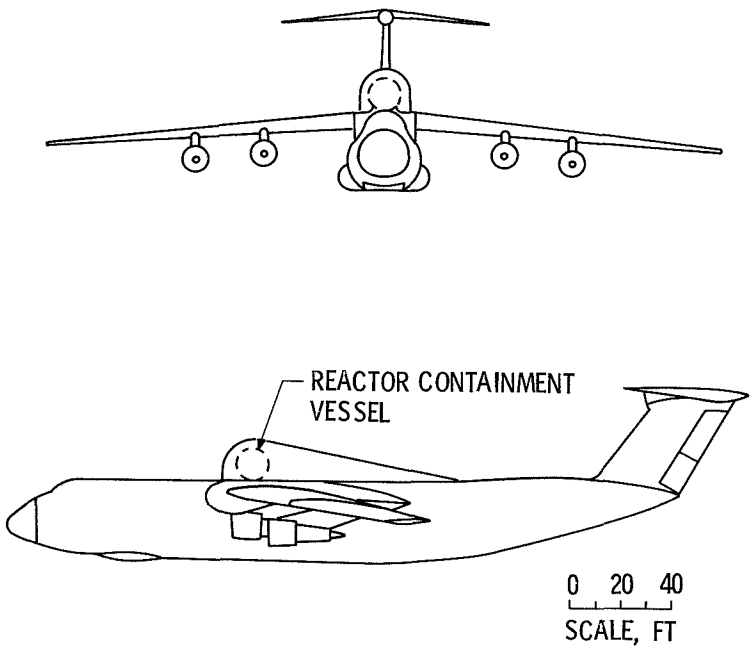

Figure 1. - C5-A aircraft.

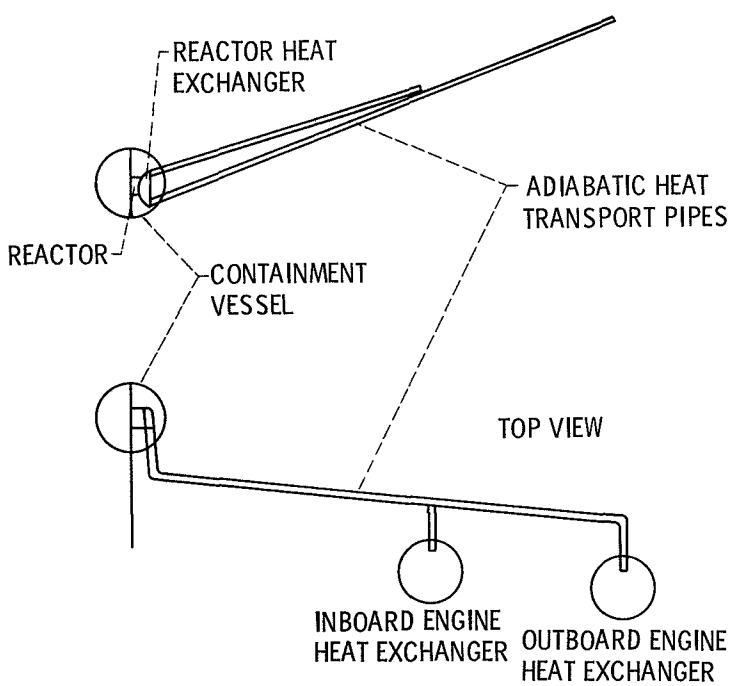

Figure 2. - Elements of reactor-to-jet engine heat pipe heat transport system.

E-5650

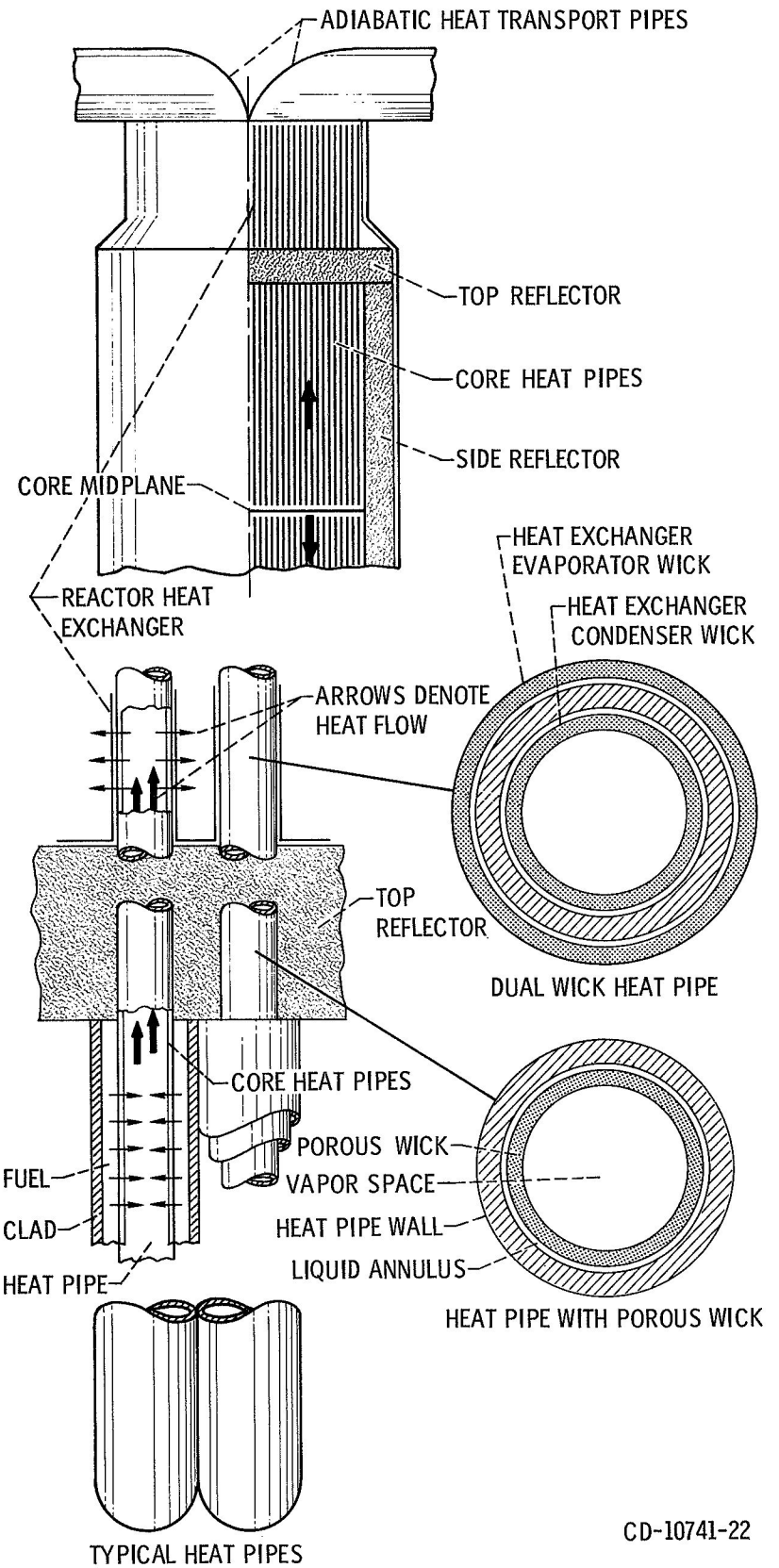

Figure 3. - Reactor and reactor heat exchanger configuration.

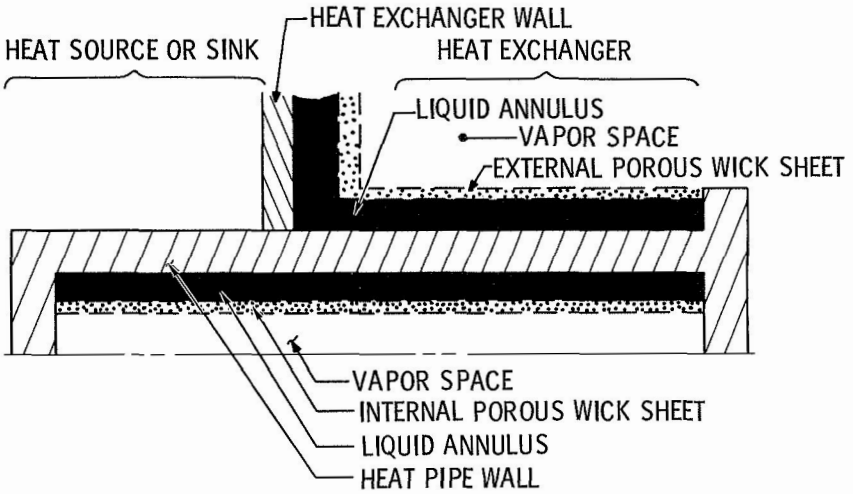

Figure 4. - Dual-wick heat pipe configuration.

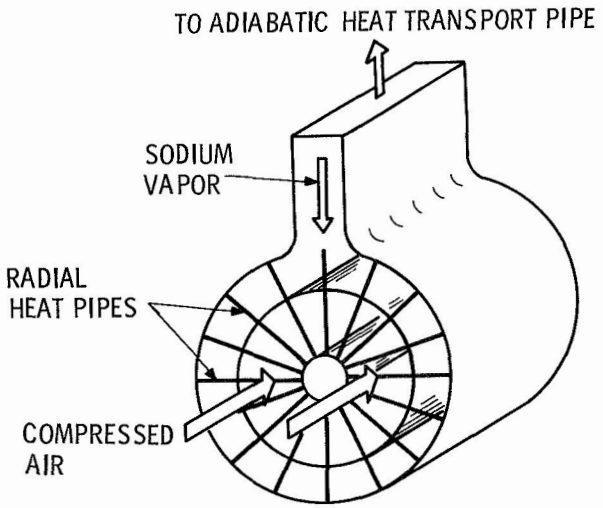

Figure 5. - Engine heat exchanger configuration.

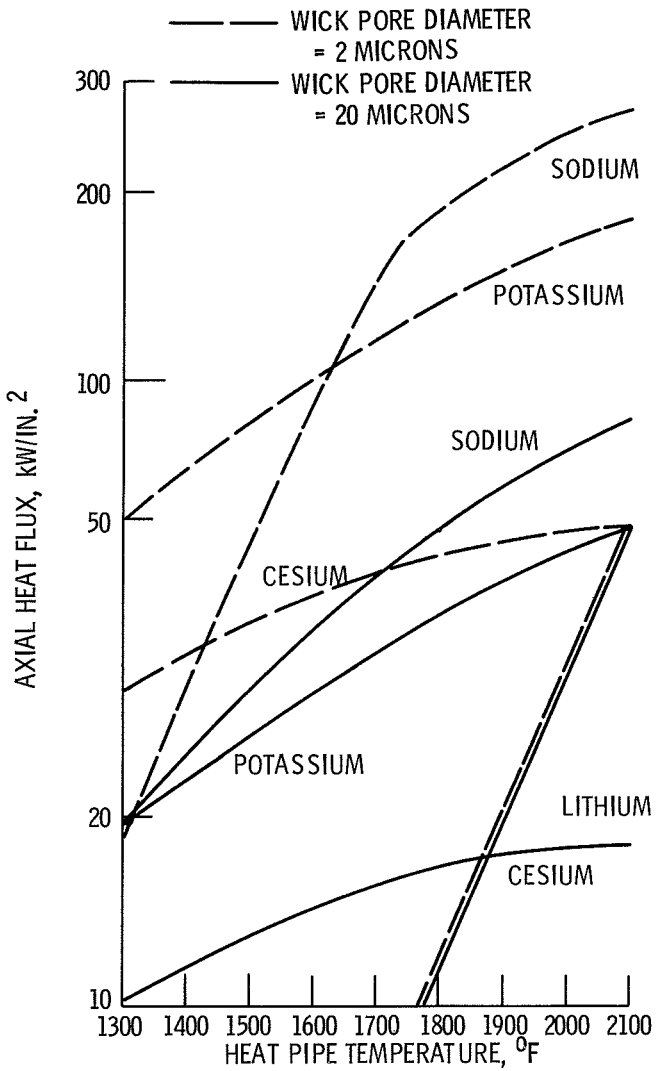

Figure 6. - Axial heat flux for no entrainment and evaporator temperature drop of 20° F or less.

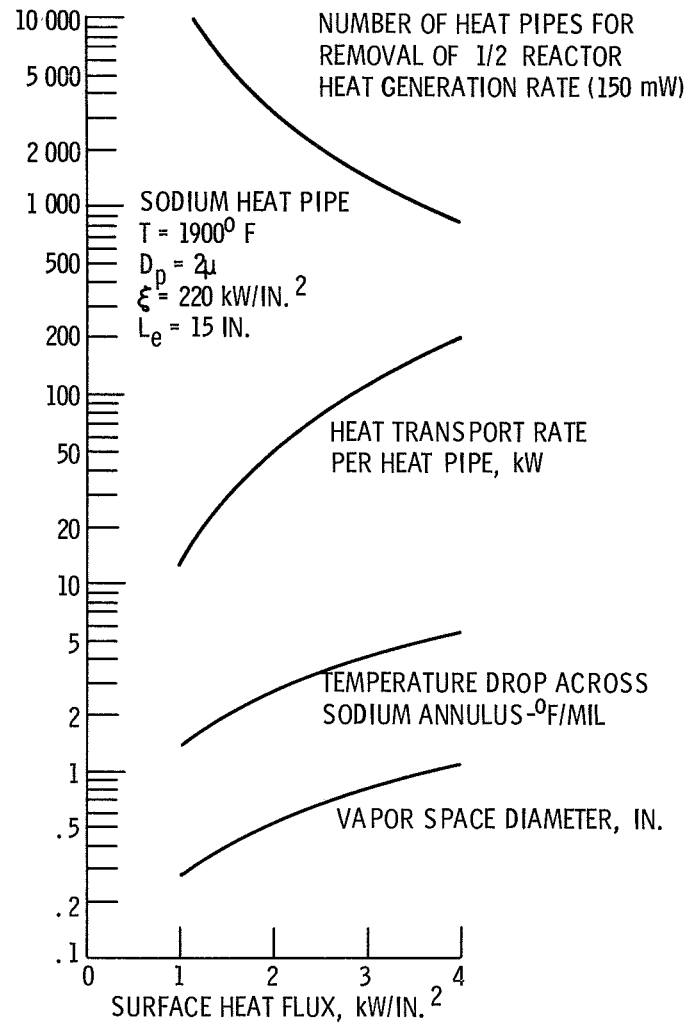

Figure 7. - Variation of heat pipe parameters with surface heat flux.

E-5650

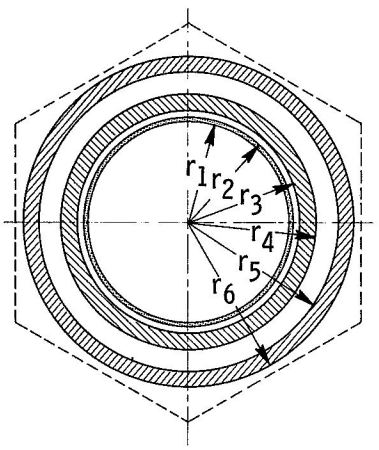

r	RADIUS		$R_i - R_{i-1}$		MATERIAL	DENSITY		AREA		$\rho N_o/A$	
	IN.	CM	IN.	CM		LB/IN.^{3}	GM/CC	IN.^{2}	CM^2		
1	0.250	0.635	-----	------	NA	0.0406×10^{-3}	0.112×10^{-2}	0.1962	1.26	0.295×10^{20}	VAPOR SPACE
2	.255	.647	0.005	0.0127	TZM	.258	7.16	.00795	.0512	$.0448 \times 10^{24}$	WICK
3	.265	.673	.010	.0254	NA	.0255	.971	.0157	.1018	$.0254 \times 10^{24}$	LIQUID SPACE
4	.298	.757	.033	.084	TZM	.369	10.22	.0598	.388	$.0640 \times 10^{24}$	PIPE
5	.373	.947	.075	.190	UN	.492	13.60	.160	1.038	$.0325 \times 10^{24}$	FUEL
6	.408	1.035	.035	.089	TZM	.369	10.22	.086	.554	$.0640 \times 10^{24}$	CLAD

Figure 8. - Proposed design of heat pipes in reactor.

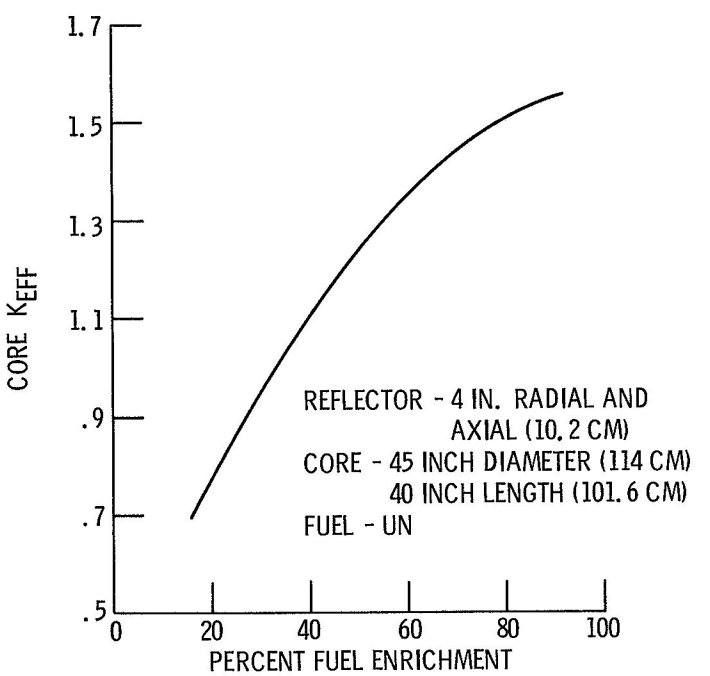

Figure 9. - Core K_{EFF} as function of percent fuel enrichment.

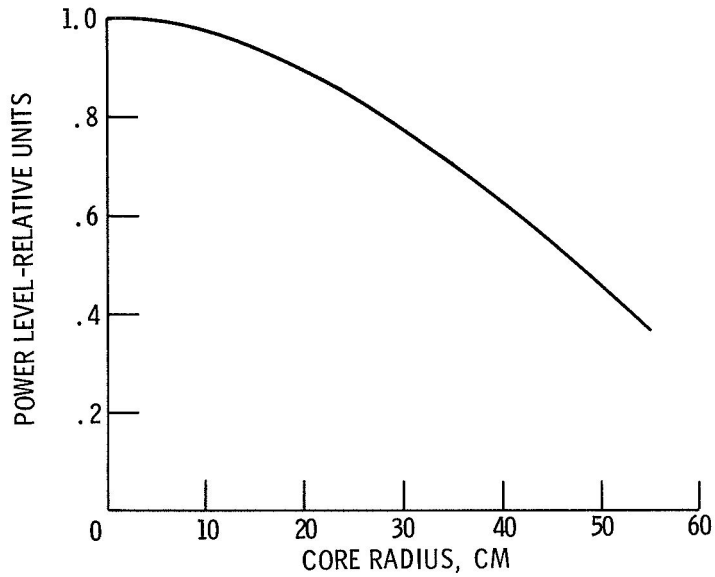

Figure 10. - Power level as function of core radius.

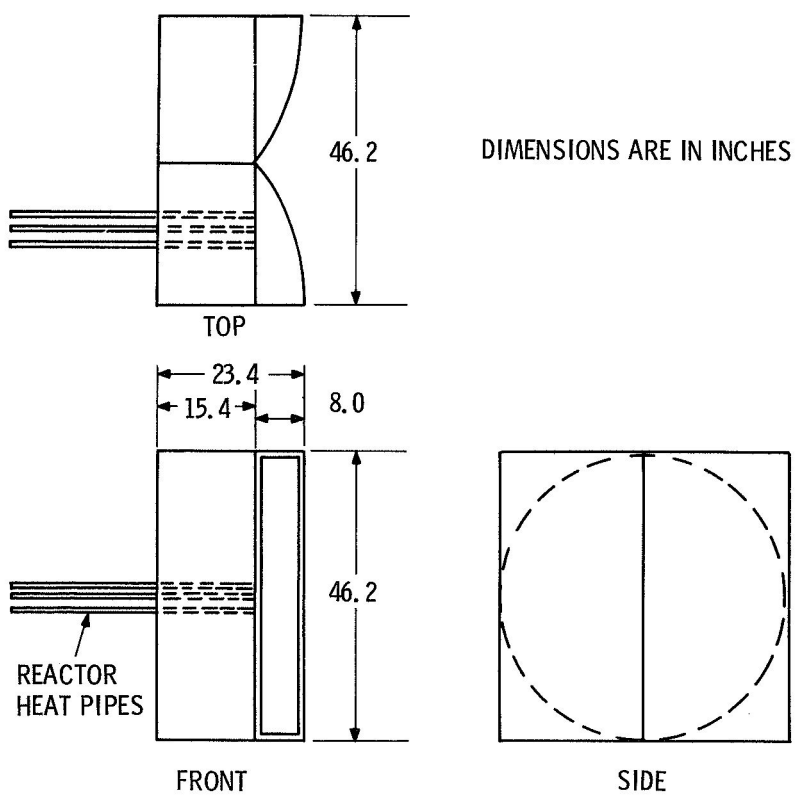

Figure 11. - Reactor heat exchanger enclosure.

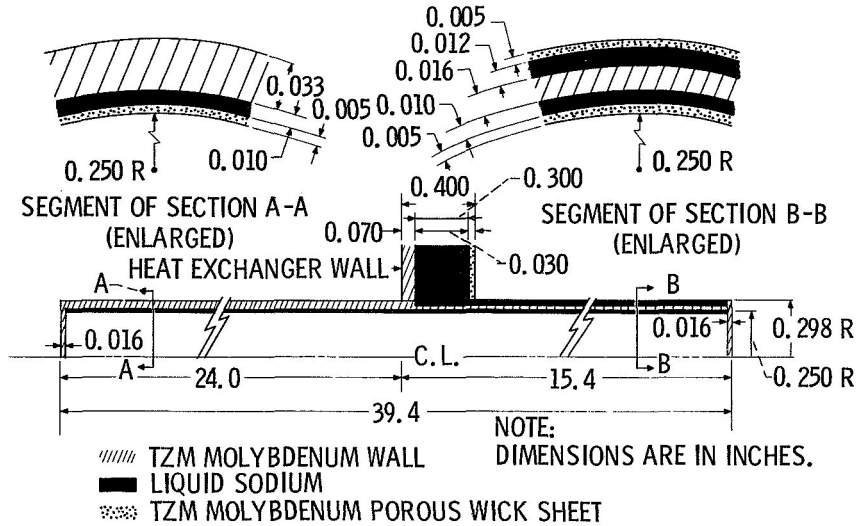

Figure 12. - Heat pipe design for reactor heat exchanger.

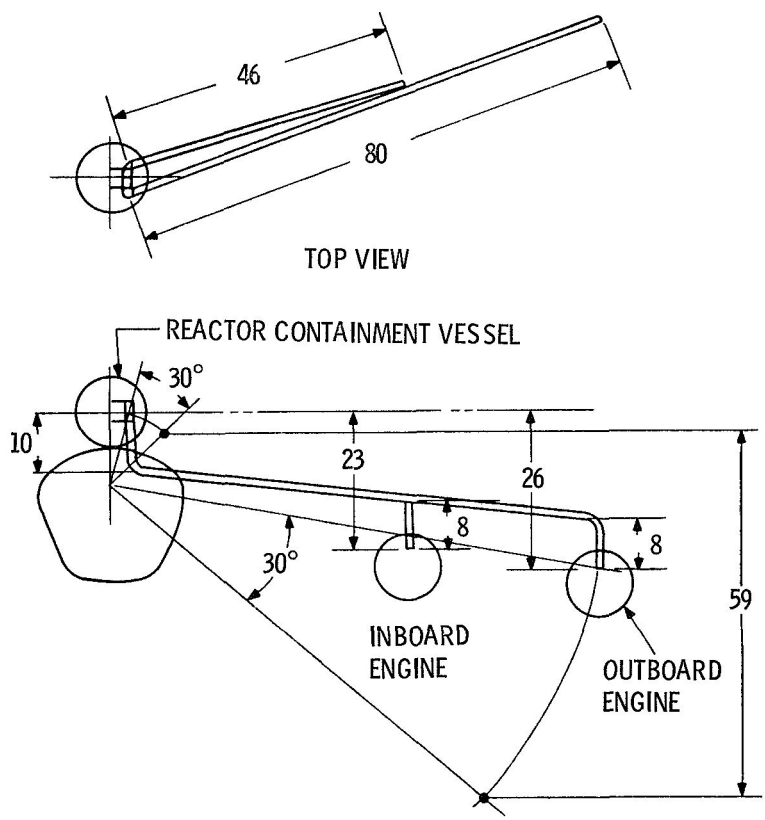

Figure 13. - Elevations and distances between major system components.

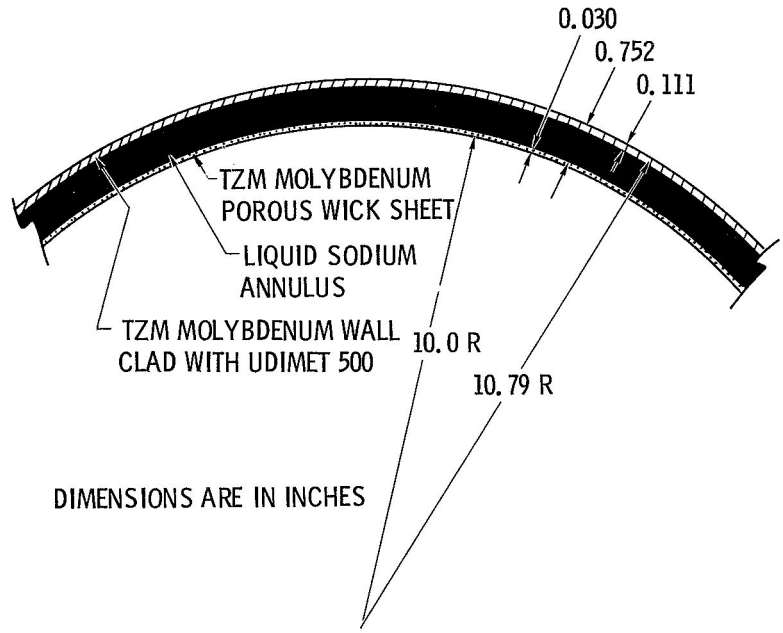

Figure 14. - Segment of adiabatic heat transport pipe cross-section.

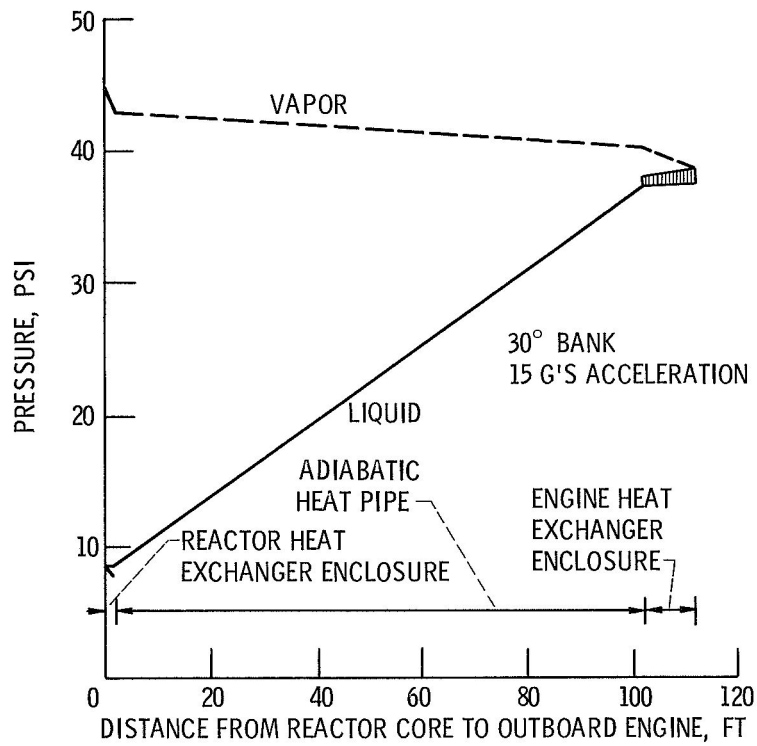

Figure 15. - Pressure distribution in adiabatic heat transport pipe fluid.

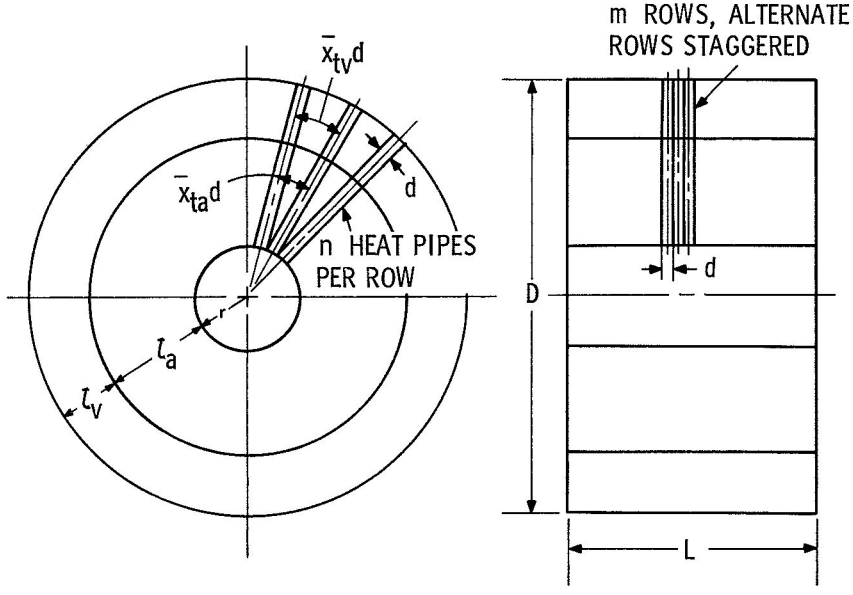

Figure 16. - Engine heat exchanger geometric parameters.

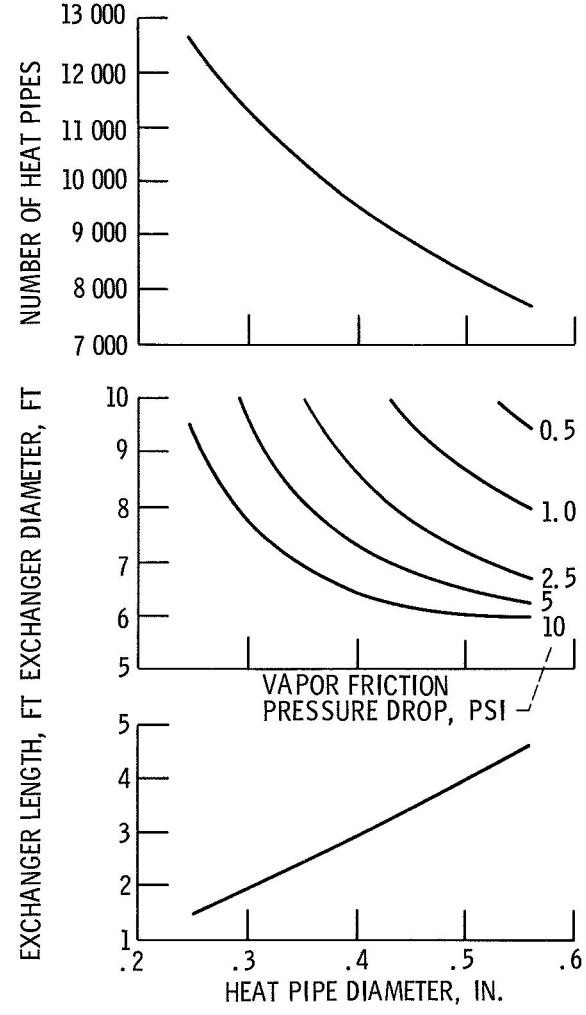

Figure 17. - Engine heat exchanger dimensions and number of heat pipes versus heat pipe diameter.

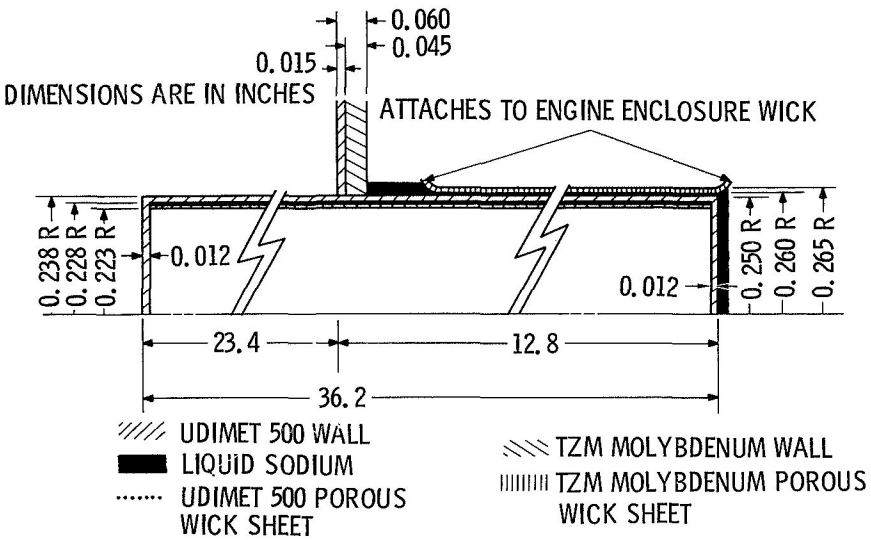

Figure 18. - Heat pipe for engine heat exchanger.

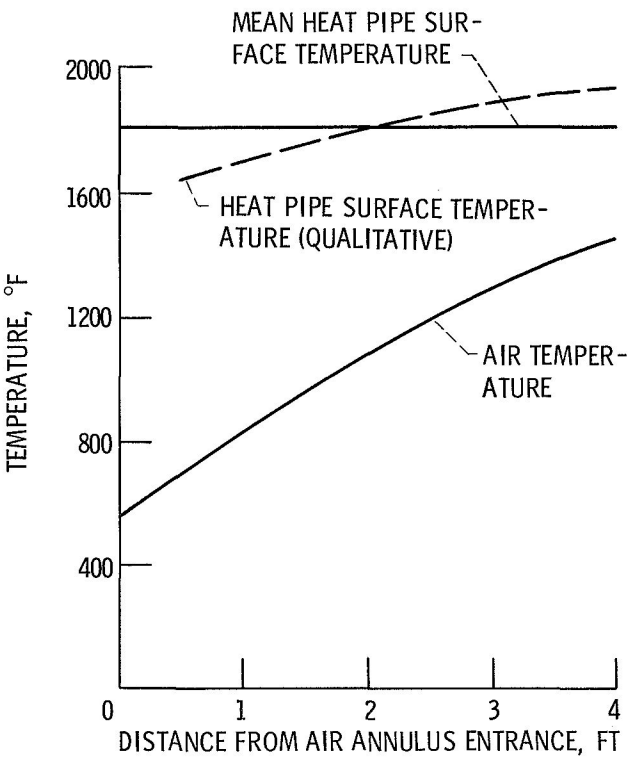

Figure 19. - Temperature distribution along air annulus of engine heat exchanger.